



HAL
open science

Ultrafast Dynamics of Fully Reduced Flavin in Catalytic Structures of Thymidylate Synthase ThyX

Nadia Dozova, Fabien Lacombat, Murielle Lombard, Djemel Hamdane, Pascal Plaza

► **To cite this version:**

Nadia Dozova, Fabien Lacombat, Murielle Lombard, Djemel Hamdane, Pascal Plaza. Ultrafast Dynamics of Fully Reduced Flavin in Catalytic Structures of Thymidylate Synthase ThyX. *Physical Chemistry Chemical Physics*, 2021, 23, pp.22692-22702. 10.1039/D1CP03379D . hal-03361405

HAL Id: hal-03361405

<https://hal.science/hal-03361405>

Submitted on 1 Oct 2021

HAL is a multi-disciplinary open access archive for the deposit and dissemination of scientific research documents, whether they are published or not. The documents may come from teaching and research institutions in France or abroad, or from public or private research centers.

L'archive ouverte pluridisciplinaire **HAL**, est destinée au dépôt et à la diffusion de documents scientifiques de niveau recherche, publiés ou non, émanant des établissements d'enseignement et de recherche français ou étrangers, des laboratoires publics ou privés.

PCCCP

Physical Chemistry Chemical Physics

Accepted Manuscript

This article can be cited before page numbers have been issued, to do this please use: N. Dozova, F. Lacombat, M. Lombard, D. Hamdane and P. Plaza, *Phys. Chem. Chem. Phys.*, 2021, DOI: 10.1039/D1CP03379D.



This is an Accepted Manuscript, which has been through the Royal Society of Chemistry peer review process and has been accepted for publication.

Accepted Manuscripts are published online shortly after acceptance, before technical editing, formatting and proof reading. Using this free service, authors can make their results available to the community, in citable form, before we publish the edited article. We will replace this Accepted Manuscript with the edited and formatted Advance Article as soon as it is available.

You can find more information about Accepted Manuscripts in the [Information for Authors](#).

Please note that technical editing may introduce minor changes to the text and/or graphics, which may alter content. The journal's standard [Terms & Conditions](#) and the [Ethical guidelines](#) still apply. In no event shall the Royal Society of Chemistry be held responsible for any errors or omissions in this Accepted Manuscript or any consequences arising from the use of any information it contains.

Ultrafast Dynamics of Fully Reduced Flavin in Catalytic Structures of Thymidylate Synthase ThyX

Nadia Dozova,^a Fabien Lacombar,^a Murielle Lombard,^b Djemel Hamdane*^b and Pascal Plaza*^a

^a PASTEUR, Département de chimie, École normale supérieure, PSL University, Sorbonne Université, CNRS, 75005 Paris, France.

^b Laboratoire de Chimie des Processus Biologiques, CNRS-UMR 8229, Collège de France, Sorbonne Université, 75005 Paris, France.

† Electronic supplementary information (ESI) available. See DOI:

ABSTRACT

Thymidylate is a vital DNA precursor synthesized by thymidylate synthases. ThyX is a flavin-dependent thymidylate synthase found in several human pathogens and absent in humans, which makes it a potential target for antimicrobial drugs. This enzyme methylates the 2'-deoxyuridine 5'-monophosphate (dUMP) to 2'-deoxythymidine 5'-monophosphate (dTMP) using a reduced flavin adenine dinucleotide (FADH⁻) as prosthetic group and (6R)-N₅,N₁₀-methylene-5,6,7,8-tetrahydrofolate (CH₂THF) as a methylene donor. Recently, it was shown that ThyX-catalyzed reaction is a complex process wherein FADH⁻ promotes both methylene transfer and reduction of the transferred methylene into a methyl group. Here, we studied the dynamic and photophysics of FADH⁻ bound to ThyX, in several substrate-binding states (no substrate, in the presence of dUMP or folate or both) by femtosecond transient absorption spectroscopy. This methodology provides valuable information about the ground-state configuration of the isoalloxazine moiety of FADH⁻ and the rigidity of its local environment, through spectra shape and excited-state lifetime parameters. In the absence of substrate, the environment of FADH⁻ in ThyX is only mildly more constrained than that of free FADH⁻ in solution. The addition of dUMP however narrows the distribution of ground-state configurations and increases the constraints on the butterfly bending motion in the excited state. Folate binding results in the selection of new ground-state configurations, presumably located at a greater distance from the conical intersection where excited-state decay occurs. When both substrates are present, the ground-state configuration appears on the contrary rather limited to a geometry close to the conical intersection, which explains the relatively fast excited-state decay (100 ps on the average), even if the environment of the isoalloxazine is densely packed. Hence, although the environment of the flavin is dramatically constrained, FADH⁻ retains a

dynamic necessary to shuttle carbon from folate to dUMP. Our study demonstrates the high sensitivity of FADH⁻ photophysics to the constraints exerted by its immediate surroundings.

1. INTRODUCTION

2'-deoxythymidine 5'-monophosphate (dTMP) is an essential biomolecule since it forms one of the four building blocks of DNA. This precursor results from the reductive methylation of the C₅ carbon of 2'-deoxyuridine 5'-monophosphate (dUMP) catalyzed by thymidylate synthases.¹⁻⁴ Most living organisms, including humans, rely on a so-called "classical" thymidylate synthase (ThyA in *E. coli*), which uses 5,10-methylenetetrahydrofolate (CH₂THF) as both carbon donor and reducing agent, to generate dTMP from dUMP.⁵ The mechanism of classical thymidylate synthase has been very well established.⁵

Some bacteria and archaea, notably several severe pathogens, use an alternative thymidylate synthase, namely flavin-dependent thymidylate synthase ThyX, which differs in term of structure and chemical mechanism from that of the classical thymidylate synthase.⁶⁻¹⁰ For these reasons, ThyX represents a promising antimicrobial target. ThyX functions with a prosthetic group, flavin adenine dinucleotide (FAD), for activity and use NADPH, CH₂THF and dUMP as substrates to produce NADP⁺, THF and dTMP.^{1,6} Although, the chemical mechanism of ThyX has been subjected to strong debates,¹¹⁻¹⁶ recent findings^{8,17,18} suggest that ThyX may share a similar mechanism to that of the bacterial flavin-dependent tRNA methyltransferase, TrmFO.^{17,19} The recently proposed chemical mechanism of ThyX is described in Fig. 1. The first step consists of the reduction of oxidized FAD (FAD_{ox}) by NADPH leading to the flavin hydroquinone (FADH⁻), which is then used as a mediator in the transfer of methylene from CH₂THF to dUMP. In particular, a flavin carbinolamine, which could be in equilibrium with its iminium counterpart, is formed transiently during the carbon transfer reaction. The reaction ends with the reduction of the nucleotidic methylene by FADH⁻, thereby converting the dUMP into dTMP and recovering the initial FAD_{ox}. Thus, the flavin acts as both a carbon and hydride transfer agent in a unique reactivity.

This flavin chemistry is supported by a series of crystallographic structures of oxidized ThyX from *Thermotoga maritima* (*TmThyX*) in complex with its substrates,^{1,20} and by the recent crystal structure of the flavin carbinolamine intermediate in *TmThyX*.¹⁸ In the free form (pdb 1O2A), *TmThyX* exhibits two large cavities bordering the two opposite faces (*re* and *si*) of the isoalloxazine (Fig. 2A). The presence of positively charged R₇₈ placed in front of N₁-FAD is likely to stabilize the negatively charged FADH⁻ species.

The nucleotidic substrate binds to the *si*-side of FAD in which lies the conserved R₁₇₄ residue, essential for dUMP activation (pdb 1O26, Fig. 2B).^{14,16} The most compelling evidences regarding the role of flavin as a mediator in the carbon transfer reaction is provided by the structure of *TmThyX* in complex with both dUMP and CH₂THF (Fig. 2D).²⁰ In this structure (pdb 4GT9), the substrates adopt a stacked configuration where the planar isoalloxazine ring of FAD_{ox} is sandwiched between CH₂THF and dUMP. The pterin moiety of CH₂THF is also sandwiched between the *re*-face of the isoalloxazine and the imidazole ring of His₅₃, which is again a shared folate-binding feature with TrmFO.²¹ Most importantly, the reactive N₅ nitrogen of FAD_{ox} is ideally poised to shuttle the CH₂ from CH₂THF to C₅-dUMP. In the structure with the carbinolamine adduct, the isoalloxazine adopts a butterfly conformation, significantly bent along its C_{10a}-C_{4a} axis and its N₅ is pyramidal, consistent with an sp³ hybridized nitrogen and alkylation of N₅.¹⁸ Furthermore in this structure, the methylene group of the carbinolamine adduct seems properly oriented for S_N2 attack by the activated nucleobase to generate an intermolecular C-C bond, leading to the FAD-CH₂-dUMP intermediate (Fig. 1). Finally, the structure of a *TmThyX* mutant (E144R) complexed with CH₂THF only shows that the folate can also bind in the dUMP-binding site (pdb 4GTE). However, in this configuration, the methylene moiety is too far from the N₅-FAD to allow any carbon transfer (Fig. 2C).²⁰ In addition, CH₂THF affects the binding of the isoalloxazine, which is repelled from its initial position observed in all *wild-type* structures of ThyX. It should also be noted that the (p-aminobenzoyl)-glutamate moiety of CH₂THF is not visible indicating a significant mobility of this chemical group. Hence, the folate-binding site observed in this mutant is most likely non-functional.

Although, the structures of oxidized *TmThyX* offer insights into mechanistic perspectives of flavin-dependent thymidylate biosynthesis, the oxidized flavin is not catalytically active. Furthermore, the mere proximity of the reactive N₅ FAD_{ox} nitrogen with both substrates is not sufficient since some dynamics of FADH⁻ is expected to occur, namely an inversion of the configuration of its N₅ nitrogen, to allow the transfer of the carbon from the folate present at the *re*-face to dUMP lying at *si*-face of the isoalloxazine. Interestingly, in the flavin monooxygenase *RutA*, such a type of N₅ nitrogen inversion has also been invoked to allow the transfer of activated oxygen from the *re*-side to the *si*-side of FAD where the uracil substrate is bound.²² Unfortunately, the structure of reduced ThyX and the involvement of FADH⁻ dynamic relevant to the catalysis are still missing. More generally, the effect of substrate(s) on the photodynamic of flavin in reduced flavoenzymes has not been studied so far. In fact, nitrogen inversion could be promoted by the peculiar structure of the FADH⁻ isoalloxazine ring, which unlike FAD_{ox}, can adopt various bent conformations (see below).

In the present work, we attempted to gain some additional insights about the configuration of the isoalloxazine in catalytically-relevant situations by using the photophysical properties of FADH⁻ itself.

The photophysics of FAD_{ox} has been used in numerous studies of flavoproteins.²³⁻³² The guiding principle is that electronic excitation of the oxidized isoalloxazine makes it prone to be reduced by suitable electron donors placed at short distance.³³⁻³⁵ Ultrafast electron transfer from close-lying aromatic aminoacids to excited FAD_{ox} has indeed been observed in many flavoproteins.²³⁻²⁷ Using the theory of electron transfer,^{36,37} one may relate the rate of electron transfer to the distance between the electron donor and the flavin.³⁸ This property has been used to show that the active site of *TmThyX* is highly flexible in the absence of substrate and that binding of dUMP abolishes this flexibility.²⁸ Yang *et al.* have similarly probed ångström-scale structural changes in a single flavin reductase molecule.³⁹

Using FADH⁻ instead of FAD_{ox} is much a less widespread approach although the properties of this species are quite interesting. FADH⁻ in aqueous solution undergoes very fast (multiexponential) excited-state decay (in the range of 8-25 ps).^{34,40-44} This decay however becomes much slower (0.6-3 ns) when the flavin is imbedded in a protein environment,⁴⁵⁻⁵¹ which makes the fluorescence of this species readily detectable as is also the case in rigid glasses at 77 K.⁵² This behavior is related to the geometry of the reduced isoalloxazine, which is bent along the N₅-N₁₀ short axis, as concluded by different NMR measurements^{53,54} and theoretical calculations.⁵⁵⁻⁶⁴ The bend angle ranges between 8° and 28° depending on the source and is strongly affected by the environment of the molecule (protic solvent, rigid protein), some lower values (2-18°) being reported inside several reduced flavoproteins.⁶⁵⁻⁶⁷ This is well understood given the low barrier to ring inversion (2-4.8 kcal/mol^{54-56,58}), also called butterfly motion, between two bent configurations of the isoalloxazine (edge pointing toward the re or si face), with the N₁₀-substituent and N₅-H atom lying either in the equatorial plane or in axial position.^{42,54} Within this context, continuous motion along the butterfly bending coordinate, leading to a conical intersection (CI) with the ground state, has been proposed to explain the rapid excited-state decay of FADH⁻ in solution.^{34,43,44} In the more rigid environment of certain flavoproteins, this motion is supposed to be hindered, thereby explaining the much enhanced excited-state lifetime.⁴⁹ It has alternatively been proposed that the existence of different conformers, differing by their degree of planarity, and reduced to one in rigid environment, could explain the fast non-exponential decay of the excited state in fluid solution.^{40,42} Little is known about the actual geometry of the CI. Ai *et al.*⁶⁸ calculated for FADH⁻ in vacuum a CI with pronounced out-of-plane bending of the phenyl ring, pyramidalization at C_{9a} and extension of C_{9a}-N₁₀ and C_{9a}-C₉ bonds. Gozem *et al.*⁶⁹ similarly calculated a highly distorted CI in the deactivation pathway of a N₅-alkylated 4a-hydroxy flavin.

Here we present a study, performed by femtosecond transient absorption spectroscopy, of the photophysics of FADH⁻ in *TmThyX* in four situations: free of substrates, in complex with dUMP or with the catalytically inactive analogue of CH₂THF, 5-methyltetrahydrofolate (CH₃THF) and reduced *TmThyX* in complex with both dUMP and CH₃THF. The latter was chosen as it is the closest folate derivative to CH₂THF and differs from it by only one hydride. The advantage of substituting CH₂THF by CH₃THF is to avoid the reaction of carbon transfer from folate to flavin. The interest of these four systems is double. They first materialize enzymatically-relevant intermediates in the catalytic cycle, following the flavin reduction and preceding the carbon transfer step. They additionally implement different environments of the reduced flavin, with variable constraints exerted on its isoalloxazine moiety. We thereby aim at evaluating the ability of FADH⁻ to sense these constraints and reciprocally inform on the impact of the different substrates on its structure. Our results are discussed within the context of the enzymatic activity of ThyX.

2. MATERIALS AND METHODS

2.1. Samples preparation

TmThyX was expressed and purified as previously described.¹⁷ The FAD-free apoprotein was prepared by treating *TmThyX* with saturating amounts of NaCl in the presence of buffer solution of 20 mM Tris-HCl, pH 8.0; 2 mM 2-mercaptoethanol until precipitation. The solution was then centrifuged at 13,000 rpm. The precipitated protein was washed several times with saturated NaCl solution and then dissolved in 20 mM Tris-HCl, pH 8.0; 2 mM 2-mercaptoethanol buffer. The sample was then loaded on a superdex-S200 (GE) equilibrated with a 50 mM sodium phosphate pH 8, 100 mM L-arginine and 1 mM ethylenediaminetetraacetic acid (EDTA). Further buffer exchange was carried out with a Pd10 column.

FADH⁻ (0.1 M, phosphate buffer at pH 8) was prepared by reducing FAD_{ox} (Sigma-Aldrich) by adding stoichiometric quantities of sodium dithionite.^{17,42,52} Steady-state absorption spectroscopy was used to monitor the titration and stop the reaction at the equivalence point.

All samples containing *TmThyX* were prepared in phosphate buffer (0.1 M) at pH 8, with 10% glycerol in anaerobic conditions. The *TmThyX* monomer concentration was here chosen in slight excess (1.25 times) of the flavin concentration (0.4 to 0.55 mM), which should guaranty full complexation of the flavin. dUMP and CH₃THF were used in larger excess (8-12 times). ThyX is known to bind dUMP with a dissociation constant of 0.03 μM and CH₂THF or both dUMP and CH₂THF with dissociation constants of the same order of magnitude.^{2,14,16} The flavin concentration was measured by recording the steady-state

absorption spectra of identical mixtures devoid of ThyX (not shown). At a practical level, apo-*TmThyX* was added to solutions of FADH⁻ containing CH₃THF (Eprova, Switzerland) or dUMP (Sigma-Aldrich) and CH₃THF. In the case of the complex with dUMP, the flavin and dUMP were added to the protein solution, to avoid precipitation. The incorporation of FADH⁻ and the complexation of the two substrates was confirmed by steady state spectroscopy (see details in Section 3.1).

Steady-state absorption spectra were measured with a CARY 300 (Varian) double-beam spectrophotometer. The samples were kept at 10 °C with the help of a circulating thermostat bath.

2.2. Femtosecond transient absorption spectroscopy

Transient absorption spectra were recorded by the pump-probe technique, with a white-light continuum probe, as previously described.^{70,71} The pump pulses (50 fs) were tuned at 360 nm by sum frequency of a beam at 810 nm taken from the amplified fs laser (Tsunami+Spitfire, Spectra-Physics) and a beam at 648 nm produced in a non-collinear optical parametric amplifier (NOPA, Clark MXR). The energy used to excite the samples was ~70 nJ per pulse, focused on a surface of ~11600 μm² (at half of maximum). It was checked by varying the excitation energy that the working energy lies in the linear regime. The excited fraction of the samples was calculated by using a previously detailed⁷² method using the transient absorption spectra of the [Ru(bpy)₃]²⁺ complex⁷³ recorded under the same conditions: the excited fraction was found to be in the order of 1-2%.

The samples were kept in 1-mm-path, fused silica, anaerobic screw cap cells (Hellma), continuously moving in two dimensions to avoid consecutive irradiation of the same volume. Experiments were performed at 10 °C, and steady-state absorption spectra were regularly recorded to check that no degradation of the samples occurred.

The polarizations of the pump and probe beams were set at the magic angle, to eliminate any contribution of rotational diffusion to the signals. The transient absorption spectra (ΔA) were corrected from the chirp of the probe beam, independently measured by recording cross-phase modulation⁷⁴ (XPM) in the pure solvent.

2.3. Data analysis

The transient absorption data were globally fitted⁷⁵ to a sum of exponential functions, in cases followed by a small plateau, convoluted by a Gaussian function representing the instrument response function (~100 fs, full width at half maximum). Singular value decomposition⁷⁶ was applied to reduce the dimensionality to the data, filter out noise and ease the fitting procedure. The global fits yield time

constants and spectra of pre-exponential factors, called decay-associated difference spectra (DADS; presented in ESI[†]). The latter were used to build so-called evolution-associated difference spectra (EADS),⁷⁵ which correspond to a virtual cascading model with unit quantum yield between successive states and summarize the dynamics of the data (see example of free FADH⁻ in aqueous solution, detailed in ESI,† Section S1).

As will be seen below, the dynamics of the transient absorption data reflects both the evolution of the transient population on the excited-state surface and the decay of this population from the excited-state surface. In order to focus as much as possible on the excited-state decay, we integrated the transient spectra between 380 and 700 nm to smooth out the spectral changes occurring while the transient population evolves on the excited-state surface. The obtained kinetic traces were fitted to sum of exponentials (parameters in Table 2). The average decay time ($\bar{\tau}$) and standard deviation of decay times (σ) were finally calculated (values in Table 3) using the fitted parameters. The procedure is detailed in ESI,† Section S1.3 with the representative example of free FADH⁻ in solution.

3. RESULTS AND DISCUSSION

3.1. Steady-state absorption spectroscopy

Fig. 3 shows the steady-state absorption spectra of reduced *TmThyX* (*i.e.* bearing FADH⁻), noted rX, and rX complexed with dUMP (rXd), with CH₃THF (rX5) and with both dUMP and CH₃THF (rXd5). The spectra of rXd, rX5 and rXd5 are consistent with previously published spectra of complexes with dUMP and CH₂THF,^{14,16} which confirms the correct binding of the substrates. The spectrum of free FADH⁻ in solution is given for reference (dotted line). For mutual comparison, all spectra are presented in molar extinction coefficient units (ϵ) relative to the flavin concentration.

The absorption spectrum of free FADH⁻ exhibits a characteristic weakly structured sloping shape, decreasing towards zero by 500 nm.^{52,63,77,78} In their seminal work, Ghisla *et al.*⁵² established that the absorption of reduced flavins in the near UV and visible range is composed of three electronic transitions overlapping to various degrees. These transitions are for instance well distinguished at 415 nm (noted T₁), 356 nm (T₂) and 296 nm (T₃) for anionic reduced tetraacetyl riboflavin in ethanol at 77 K. This analysis has been supported by fluorescence polarization excitation experiments,⁴⁵ and more recently by Stark spectroscopy⁶³ as well as theoretical calculations.^{63,79} At room temperature or in reduced FMN (flavin

adenine mononucleotide) or FAD in aqueous solution, these bands are reduced to shallow structures, as observed here, presumably due to heterogeneous broadening.

The absorption spectra of our *TmThyX* systems show significant differences as compared to that of free FADH⁻. For rX, one observes that the weak structures of FADH⁻ are enhanced. A clear shoulder is in particular visible around 390 nm (T₁) and a weaker one by 345 nm (T₂). Within the context of the temperature and environment effects reported by Ghisla *et al.*,⁵² this may be interpreted by a stiffening of the flavin environment or loss of hydrogen bonds, that reduce the magnitude of inhomogeneous broadening and reveals the underlying transitions. Similar features are observed for rXd with a red shift of the transitions, T₁ being found around 415 nm and T₂ around 352 nm. The red shift of T₁ has in particular been related to the degree of planarity of the isoalloxazine ring;⁵² it can thus be here deduced that the addition of dUMP induces a partial planarization of the molecule. This is well understood referring to the crystal structure of oxidized *TmThyX* in complex with dUMP,¹ which shows a π - π stacking of the isoalloxazine and pyrimidine moiety of dUMP, both rings being nearly parallel and separated by a distance of ~ 3.5 Å (Fig. 2B). The pyrimidine moreover faces the central ring of the isoalloxazine, which should indeed favor the planarization of the flavin.

Much less binding effects are seen in the case of rX5. The absorption spectrum only shows a mild and broad shoulder around 390 nm, probably to be assigned to T₁. The spectrum of rX5 is in fact less structured than that of rX, and more similar to that of free FADH⁻ (as previously observed¹⁶), which suggest a significant change in the surroundings of the isoalloxazine, with possibly more heterogeneous broadening and loss of planarity. Although there is no structure of *wild-type TmThyX* in complex with CH₂THF, the structure of *TmThyX* E144R mutant shows that the folate can take the place of dUMP, forcing the flavin to adopt a non-canonical conformation (Fig. 2C). Furthermore, in this structure, only 2 out of 4 flavins and folates are resolved, suggesting that these molecules are highly mobile. In contrast, a very large distortion of the absorption spectrum is observed for the rXd5 complex, its T₁ transition being strongly red shifted to ~ 440 nm. By letting the sample oxidize under air, we verified that this band does not belong to FAD_{ox} (hypothetically produced by accidental exposition to air), the spectrum of which appears around 470 nm in this complex (not shown), with characteristic vibronic structures (460/483 nm) not observed in the reduced sample. The large red shift of T₁ in rXd5 suggests that binding of both dUMP and CH₃THF substrates induces an even larger planarization of the molecule than upon binding of dUMP alone. This is coherent with the crystal structure of oxidized *TmThyX* bound to both dUMP and CH₂THF (pdb 4GT9),²⁰ which shows that FAD_{ox} is sandwiched between CH₂THF and dUMP (Fig. 2D). This structure further shows that, while the isoalloxazine of FAD_{ox} and dUMP lie in almost parallel

configuration (dihedral angle of $\sim 3^\circ$), the isocytosine ring of CH_2THF is more significantly twisted relatively to the isoalloxazine plane ($\sim 18^\circ$).

Note that the absorption spectra of the rX complexes with CH_3THF are obscured below ~ 350 nm due to a large excess of folate in the solution (4 mM). The red edge of the CH_3THF absorption (hard to subtract), peaking at 290 nm,⁸⁰ is unfortunately visible in those spectra.

3.2. Transient absorption spectroscopy

3.2.1. Common features

We performed femtosecond transient absorption spectroscopy of the four *TmThyX* systems described above with excitation at 360 nm. Raw spectra at selected pump-probe delays within a time window of 3.2 ns are shown in Fig. 4. For reference, the transient spectra of FADH^- in solution (phosphate buffer at pH 8), in agreement with previously reported ones,^{40,42-44} are recalled in ESI,† Fig. S1.

Globally, the transient spectra of the *TmThyX* systems show similar features as those of FADH^- in solution, namely two positive bands located at around 390 nm (TA_1), with more or less marked substructures (e.g. local peaks at 375 and 410 nm for rX), and around 530 nm (TA_2), with more or less extended and structured red wing (towards 700 nm). This overall shape likely results from the superposition of a purely positive and dominant transient absorption contribution covering the whole spectrum and two negative contributions, coming from ground-state bleaching below ~ 500 nm (particularly intense below 400 nm; see Fig. 3) and stimulated emission, possibly lying around 450 nm where a marked dip is observed. Unfortunately no reliable recording of the steady-state fluorescence spectra could be made, due to the weakness of the signal. The major differences between the different complexes lie (i) in the shape of the TA_2 band and its evolution during the first picoseconds and (ii) in the excited-state decay rate. We used multiexponential global analysis (see Section 2.3) to characterize these evolutions. The results are gathered in Table 1 (time constants) and Fig. 5 (EADS); the corresponding DADS are available in ESI,† Fig. S4. For convenience, the EADS are also presented in normalized form (at the maximum of the TA_2 band) in Fig. S5 and compared to each other in Fig. S6 (ESI,† Section S2.2).

3.2.2. Interpretative background

We will essentially follow interpretations of the transient absorption spectra of FADH^- in aqueous solution reported earlier in the literature,^{34,43,44} and briefly recalled in the Introduction. For the sake of comparison, we propose here in ESI,† Section S1 (unpublished) transient spectra of FADH^- in solution, recorded under the same experimental conditions as for the *TmThyX* complexes and analyzed with the same tools.

The first issue is the initial evolution of the TA₂ band, which in the case of FADH⁻ in solution is a narrowing of the band on its red side (loss of a shoulder around 595 nm), with a slight blue shift of its maximum (Fig. S1). It takes here place mostly in 0.27 ps, with a smaller component of 1.5 ps (Fig. S2B). It has been interpreted as a relaxation of the excited state, coming in part from the response of water molecules (possibly also buffer constituents) to the change of electronic distribution in the excited state.^{81,82} It is also possible that the nonplanar configuration of the isoalloxazine undergoes some primary reshuffling, also driven by the change of charge distribution. Pauszek *et al.* later proposed that it could also be due to S₂→S₁ relaxation when the T₂ transition is excited.⁶³ This interesting hypothesis applies both to the present results with excitation at 360 nm and an experiment formerly published with excitation at 387.5 nm,⁴³ since both wavelengths likely overlap the T₂ transition. One would however expect that excitation at 360 nm favors transition T₂ and that the magnitude of the S₂→S₁ relaxation would consequently be more important. The difference between both experiments at this level is nonetheless not obvious. Furthermore, the transient spectra of FADH₂ in aqueous solution (unpublished⁸³) which are very similar to those of FADH⁻, display almost no ultrafast relaxation of the TA₂ band even though the absorption spectra are relatively comparable^{52,78} and the T₂ transition is also excited at 387.5 nm. From these elements we deduce that S₂→S₁ relaxation likely does not contribute substantially to the evolution of the transient absorption spectra in the first picoseconds, possibly because it is faster than our time resolution (~100 fs).

The second issue is the excited-state decay, which for FADH⁻ in solution is here seen to occur in 1.5, 8.4 and 32 ps. This multiexponential decay has been interpreted as coming from the motion of the system along the butterfly bending coordinate towards a conical intersection (CI) with the ground state.^{34,43,44} Multiexponentiality arises from the distribution and spread of configurations along this coordinate and possibly spatial extension of the CI seam. The original CI model³⁴ does not explicitly specify if this movement is strictly continuous along a barrierless pathway or if some small potential energy barrier needs to be crossed before reaching the CI. The barrierless view however seems reasonable given the nonexponentiality of the excited-state decay (substantial barriers would likely favor precursor-successor relationships, with simpler kinetics). Let us mention at this respect that Gozem *et al.*⁶⁹ calculated a barrierless pathway to the CI in the N₅-alkylated 4a-hydroxy flavin they studied. Within that framework, we did not seek any precise meaning for each of the time constants produced by global analysis. As explained in Section 2.3, we alternatively characterized the overall excited-state decay with the integral decay trace (Fig. 6), of which we provide the parameters of a multiexponential analysis (Table 2) and the corresponding average decay time and standard deviation of decay times ($\bar{\tau}$ and σ ,

Table 3). Note that σ is essentially provided for reference, to give a sense of the width of the distribution of time constants. For simplicity the discussion will be mostly restricted to $\bar{\tau}$.

3.2.3. Reduced *TmThyX* (*rX*)

For *rX*, the TA_2 band initially peaks at ~ 570 nm (EADS1, Fig. 5A) but rapidly loses intensity on its red edge and shifts to ~ 540 nm (EADS2) with a time constant of 0.26 ps. This shift and narrowing continues to a smaller extent during the next phase of 2.5 ps, the TA_2 band finally peaking at 535 nm. This phenomenon corresponds well to the early phase observed for $FADH^-$ in aqueous solution⁴³ (see above and ESI,[†] Section S1). The same interpretation is retained here, namely a combination of response from the immediate surroundings (aminoacids or water molecules possibly standing at short distance of the flavin) and primary relaxation of the isoalloxazine configuration, driven by the change of charge distribution. Excited-state decay follows, mostly in 42 and 117 ps, without much change of spectral shape (better seen on the normalized EADS in ESI,[†] Section S2.2). A small plateau is found, possibly corresponding to some long-lived (ns) population, insufficiently resolved in this experiment. The average integral decay time ($\bar{\tau}$), excluding the plateau, is found to be 81 ps, that is, 4.2 times longer than the $FADH^-$ reference in solution. This slowing down suggests that *ThyX* provides to the isoalloxazine a mildly more rigid environment than the aqueous solution, which is consistent with the visible but moderate effect of *ThyX* binding on the steady-state absorption spectrum of $FADH^-$ (see Section 3.1 and Fig. 3). It is also in agreement with the absence of dense packing in the immediate surroundings of the isoalloxazine seen in a crystal of oxidized *TmThyX* (Fig. 2A, pdb 1O2A).¹ In fact, it was observed from the crystal structures in this work that the flavin (FAD_{ox}) could present different conformations that differ from one another by the positioning of the isoalloxazine within the large pocket of the active site. The functional relevance of these conformations has yet to be established.

3.2.4. *rX* complexed to *dUMP* (*rXd*)

The case of complex *rXd* is similar as far as spectral shape is concerned (Fig. 5B), but the fast blue shift of the TA_2 band (543 nm to 530 nm in 0.67 ps) is less marked, its initial (in EADS1) red wing being significantly reduced as compared to *rX*. The initial shape of the TA_2 band is a signature of the ground-state configuration of the isoalloxazine, instantly projected in the excited state (directly on S_1 or through S_2 via ultrafast internal conversion; see Section 3.2.2). It may then be hypothesized that the width of this band, in particular its red extension, reflects the distribution of ground-state configurations. Within this analysis grid, the introduction of *dUMP* in the binding pocket of *ThyX* would reduce the extent of ground-state configuration distribution, in agreement with the stacking of the flavin and *dUMP* described above

(Section 3.1). After the sub-ps relaxation phase, excited-state decay of rXd mostly occurs with a time constant of 135 ps, with minor components of 8.8 and 1170 ps. The integral average decay time is 218 ps, which is 11 times longer than the FADH⁻ reference. We see that the addition of dUMP further slows down the excited-state decay, by a factor of 2.2 as compared to rX. This effect is interpreted as resulting from the (further) hindering of the butterfly bending motion in the rXd complex, also in agreement with the stacking of the flavin and dUMP described above.

3.2.5. rX complexed to CH₃THF (rX5)

Quite a peculiar behavior is observed for the rX5 complex (Fig. 5C). On the one hand, the shape of the TA₂ band is much broader (EADS1) and the amplitude of its initial relaxation is smaller than in the preceding cases. The relaxed TA₂ band (in EADS2) has indeed still a large red extension, with a more pronounced shoulder around 585 nm than in rX and rXd. The time constant of this relaxation (1.5 ps) is also slightly longer than in the preceding cases. The image that emerges from these observations is that the presence of CH₃THF likely favors new configurations of the isoalloxazine in the ground state and hinders their relaxation to the same degree as for rX and rXd. It was however observed that the steady-state absorption spectrum of the rX5 complex does not show any clearly detached T₁ transition, as in rX and rXd (Fig. 3). It may then be hypothesized that the presence of CH₃THF rather favors a large distribution of configurations, explaining the broadness of both steady-state T₁ and (initial) transient TA₂ bands, and that these configurations are likely not planar since the T₁ band is apparently not red shifted. This would be consistent with the structure of oxidized *Tm*ThyX E144R mutant in complex with CH₂THF, showing a certain flexibility of the active site and in particular of the flavin, which adopts non-canonical conformations, *i.e.* different from those seen in the *wild type* enzyme (Fig. 2C). On the other hand, the excited-state decay of rX5 is relatively slow (57, 365 and 1630 ps), with an average integral decay time of 464 ps, *i.e.* 24 times slower than the FADH⁻ reference. In view of the of the preceding elements, this effect may either be interpreted as an increased hindrance exerted by the local environment on the butterfly bending coordinate of the isoalloxazine, or else a larger distance to run between the initial (relaxed) configuration and the geometry of the CI with the ground state. Although both interpretations could simultaneously contribute to various degrees, the second hypothesis has the advantage of being compatible with the mildly constrained view of the flavin environment drawn from the steady-state absorption spectrum (Section 3.1). It is incidentally not excluded that the geometry of the CI, as well as the shape of the potential energy surface along the pathway for reaching it, might depend on the exact environment of the isoalloxazine and the constraints it exerts on it; only precise theoretical calculations in the presence of controlled environments could confirm this hypothesis.

3.2.6. rX complexed to dUMP and CH₂THF (rXd5)

The final case is yet significantly different from the preceding ones. The initial TA₂ band of rXd5 (EADS1, Fig. 5D) has first a reduced red extension and undergoes a quite small ultrafast relaxation (in 0.61 ps; better seen in ESI,† Fig. S5D). This observation suggests that the dense packing of the flavin and substrates in this complex,²⁰ reduces the distribution of ground-state configurations and selects geometries that happen to be nearly relaxed in the existed state. The 2.5 ps phase is in fact here the beginning of a surprisingly fast excited-state decay, which further proceeds in 26 ps and 145 ps. In this experiment, a small constant offset was found, coming from an experimental artifact. This spurious component was removed from the DADS, EADS representations and subtracted from the integral decay. The average integral decay time is found to be 80 ps (4.2 times the FADH⁻ reference), *i.e.* nearly the same as rX. Following the interpretation key developed above, we propose that the configuration of the isoalloxazine in rXd5, which have been determined to be the most planar one of all complexes by steady-state absorption spectroscopy (Section 3.1), is close to the geometry of the CI. It could thus reach it relatively rapidly in spite of a dense environment, which would otherwise be expected to exert a large constraint on the butterfly bending motion. One may wonder if the effect of this constraint would manifest itself as the somewhat broader distribution of integral decay times found for rXd5 as compared to rX (σ = 65 ps vs. 38 ps, Table 3).

3.3. Catalytic implications

Our steady state and transient spectroscopy data can be discussed in the context of ThyX chemical mechanism. Previous enzyme kinetics studies revealed that dUMP is the first substrate to bind to ThyX followed by CH₂THF.^{3,7,84} Our data are consistent with the fact that the binding of dUMP has the consequence of promoting a more planar conformation of isoalloxazine while reducing its dynamics. In contrast, although folate binding produces a much greater effect on the dynamics of FADH⁻, this substrate does not affect planarity. This could be interpreted by non-functional conformations of the flavin induced by folate alone, which is consistent with the structural changes observed in the active site of *Tm*ThyX E144R mutant (Fig. 2C). This mode of folate binding was considered physiologically relevant, before the discovery that flavin mediates carbon transfer.²⁰ However, in this position, the CH₂ of CH₂THF is too far away to allow its attack by the nucleophilic N₅ nitrogen of FADH⁻. This phenomenon may have a physiological meaning since it would prevent a transfer of carbon to the flavin in the absence of dUMP (uncoupling reactions). Indeed, a carbon transfer, in the absence of dUMP, could lead to adverse reactions leading to an alkylation of the protein residues via the formation of formaldehyde. As a

methylene transfer mediator, the isoalloxazine should adopt suitable conformations. Thus in the presence of both substrates, the N_5 -FADH⁻ must point in the direction of the folate to allow its nucleophilic attack. Once the methylene grafted on N_5 , the latter must undergo a configuration inversion to transfer the methylene to dUMP. Although, in the rXd5 complex, the flavin adopts a more planar conformation than that observed with rXd with a geometry close to that of the CI, it retains an important dynamic probably necessary for the unidirectional transfer of carbon from folate to the flavin and then from the latter to the dUMP.

4. CONCLUSIONS

We have shown that femtosecond transient absorption spectroscopy of fully reduced FAD is very sensitive to the interactions of the isoalloxazine moiety with its local environment in the enzyme's active site. Essentially two parameters characterize those interactions: the shape of the transient absorption band around 530 nm (TA_2), notably its width and extension of the red wing, and the excited-state decay rate. The shape of TA_2 , in particular before an initial ultrafast phase (in the range of 1 ps), reveals the variety of configurations selected by the environment, typically in terms of butterfly bending angle and possibly other less obvious structural features. The excited-state decay rate informs on the other hand on the constraints exerted by the environment on the reactive coordinate (presumably the butterfly bending motion) that leads the excited state to a CI crossing back to the ground state. These elements should be regarded as complementary to the analysis of the steady-state absorption spectrum that also inform on the rigidity of the environment and degree of planarity of the isoalloxazine, in the ground state.

Applying this approach to the case of ThyX is particularly interesting because this enzyme is able to bind two different substrates: a folate derivative and dUMP. Different complexes of reduced *Tm*ThyX (rX) could be prepared, with one substrate only (rXd, rX5) or both of them (rXd5). It first appears that the environment of FADH⁻ in rX is only mildly more constrained than in solution and does not change much the configuration of the isoalloxazine. When dUMP is added (rXd), the distribution of ground-state configurations appears somewhat reduced and the constraints on the butterfly bending motion in the excited state further increased, which agrees well with a close stacking of dUMP to the isoalloxazine even in the reduced enzyme. The effects of CH₃THF binding (rX5) are significantly different. New or more diverse ground-state configurations appear that are presumably located at a greater distance from the CI, thereby explaining the relatively slow excited-state decay. This is possibly due to the folate binding

mode in rX5, which forces the flavin to adopt non-functional conformations as seen in the crystal structures of oxidized *TmThyX* E144R mutant.²⁰ When both substrates are present (rXd5), the ground-state configuration appears on the contrary rather limited to a geometry close to the CI, which explains the relatively fast excited-state decay although the environment of the isoalloxazine is densely packed.

These results indicate that, in the catalytic structure of methylene pre-transfer reaction, the reduced flavin sandwiched between the two substrates adopts a planar conformation while retaining a relative dynamic, which will be necessary to ensure its role as a carbon transfer agent. In fact, an inversion of the configuration of the N₅ nitrogen of FADH⁻ is expected to occur during the methylation reaction to allow the transfer of the carbon from the CH₂THF present at the *re*-face to dUMP lying at *si*-face of the isoalloxazine. Contrary to what was previously predicted, namely that dUMP plays a key role in the conformational flexibility of the active site of ThyX, we show here that folate by itself can bind to rX and induce a much greater effect than dUMP on the enzyme active site dynamic, even though this effect is likely attributed to non-catalytic productive binding. This could have important future consequences in targeting the folate-binding site as an effective way for enzyme inhibition. More generally, our study demonstrates the remarkable richness of the FADH⁻ photophysics under various environments. This may motivate future studies on other flavoenzyme systems with multiple substrates, as well as theoretical calculations to refine the mechanistic details.

CONFLICT OF INTERESTS

There are no conflicts to declare.

ACKNOWLEDGEMENTS

This work was supported by the Centre National de la Recherche Scientifique, Sorbonne Université as well as grants from the French National Research Agency (ANR-15-CE11-0004-01).

We thank R. Oser (Eprova, Switzerland) for providing us with samples of the reduced folate derivatives.

REFERENCES

- 1 Mathews, II, A. M. Deacon, J. M. Canaves, D. McMullan, S. A. Lesley, S. Agarwalla and P. Kuhn, *Structure*, 2003, **11**, 677-690.
- 2 S. G. Gattis and B. A. Palfey, *J. Am. Chem. Soc.*, 2005, **127**, 832-833.
- 3 Z. Wang, A. Chernyshev, E. M. Koehn, T. D. Manuel, S. A. Lesley and A. Kohen, *FEBS J.*, 2009, **276**, 2801-2810.

- 4 X. L. Zhang, J. Y. Zhang, G. Guo, X. H. Mao, Y. L. Hu and Q. M. Zou, *Protein and Peptide Letters*, 2012, **19**, 1225-1230.
- 5 C. W. Carreras and D. V. Santi, *Annu. Rev. Biochem.*, 1995, **64**, 721-762.
- 6 H. Myllykallio, G. Lipowski, D. Leduc, J. Filee, P. Forterre and U. Liebl, *Science*, 2002, **297**, 105-107.
- 7 S. Graziani, J. Bernauer, S. Skouloubris, M. Graille, C.-Z. Zhou, C. Marchand, P. Decottignies, H. van Tilbeurgh, H. Myllykallio and U. Liebl, *J. Biol. Chem.*, 2006, **281**, 24048-24057.
- 8 T. V. Mishanina, L. Yu, K. Karunaratne, D. Mondal, J. M. Corcoran, M. A. Choi and A. Kohen, *Science*, 2016, **351**, 507-510.
- 9 D. Hamdane, H. Grosjean and M. Fontecave, *J. Mol. Biol.*, 2016, **428**, 4867-4881.
- 10 H. Myllykallio, P. Sournia, A. Heliou and U. Liebl, *Front. Microbiol.*, 2018, **9**.
- 11 D. Leduc, S. Graziani, G. Lipowski, C. Marchand, P. Le Maréchal, U. Liebl and H. Myllykallio, *Proc. Natl. Acad. Sci. USA*, 2004, **101**, 7252-7257.
- 12 E. M. Koehn, T. Fleischmann, J. A. Conrad, B. A. Palfey, S. A. Lesley, I. I. Mathews and A. Kohen, *Nature*, 2009, **458**, 919-923.
- 13 T. V. Mishanina, E. M. Koehn, J. A. Conrad, B. A. Palfey, S. A. Lesley and A. Kohen, *J. Am. Chem. Soc.*, 2012, **134**, 4442-4448.
- 14 J. A. Conrad, M. Ortiz-Maldonado, S. W. Hoppe and B. A. Palfey, *Biochemistry*, 2014, **53**, 5199-5207.
- 15 T. V. Mishanina, J. M. Corcoran and A. Kohen, *J. Am. Chem. Soc.*, 2014, **136**, 10597-10600.
- 16 F. W. Stull, S. M. Bernard, A. Sapra, J. L. Smith, E. R. P. Zunderweg and B. A. Palfey, *Biochemistry*, 2016, **55**, 3261-3269.
- 17 C. Bou-Nader, D. Cornu, V. Guérineau, T. Fogeron, M. Fontecave and D. Hamdane, *Angew. Chem. Int. Ed.*, 2017, **56**, 12523-12527.
- 18 C. Bou-Nader, F. W. Stull, L. Pecqueur, P. Simon, V. Guérineau, A. Royant, M. Fontecave, M. Lombard, B. A. Palfey and D. Hamdane, *Nat. Commun.*, 2021, **12**, 4542.
- 19 D. Hamdane, M. Argentini, D. Cornu, B. Golinelli-Pimpaneau and M. Fontecave, *J. Am. Chem. Soc.*, 2012, **134**, 19739-19745.
- 20 E. M. Koehn, L. L. Perissinotti, S. Moghram, A. Prabhakar, S. A. Lesley, I. I. Mathews and A. Kohen, *Proc. Natl. Acad. Sci. USA*, 2012, **109**, 15722-15727.
- 21 H. Nishimasu, R. Ishitani, K. Yamashita, C. Iwashita, A. Hirata, H. Hori and O. Nureki, *Proc. Natl. Acad. Sci. USA*, 2009, **106**, 8180-8185.
- 22 A. Matthews, R. Saleem-Batcha, J. N. Sanders, F. Stull, K. N. Houk and R. Teufel, *Nature Chemical Biology*, 2020, **16**, 556-563.
- 23 D. P. Zhong and A. H. Zewail, *Proc. Natl. Acad. Sci. USA*, 2001, **98**, 11867-11872.
- 24 N. Mataga, H. Chosrowjan, S. Taniguchi, F. Tanaka, N. Kido and M. Kitamura, *J. Phys. Chem. B*, 2002, **106**, 8917-8920.
- 25 A. Losi, *Photochem. Photobiol.*, 2007, **83**, 1283-1300.
- 26 K. Brettel and M. Byrdin, *Curr. Opin. Struct. Biol.*, 2010, **20**, 693-701.
- 27 I. Chaves, R. Pokorny, M. Byrdin, N. Hoang, T. Ritz, K. Brettel, L.-O. Essen, G. T. J. van der Horst, A. Batschauer and M. Ahmad, *Annu. Rev. Plant Biol.*, 2011, **62**, 335-364.
- 28 S. P. Laptinok, L. Bouzahir-Sima, J.-C. Lambry, H. Myllykallio, U. Liebl and M. H. Vos, *Proc. Natl. Acad. Sci. USA*, 2013, **110**, 8924-8929.
- 29 L. Nag, P. Sournia, H. Myllykallio, U. Liebl and M. H. Vos, *J. Am. Chem. Soc.*, 2017, **139**, 11500-11505.
- 30 J. Yamamoto, P. Plaza and K. Brettel, *Photochem. Photobiol.*, 2017, **93**, 51-66.
- 31 N. Dozova, F. Lacombat, C. Bou-Nader, D. Hamdane and P. Plaza, *Phys. Chem. Chem. Phys.*, 2019, **21**, 8743-8756.
- 32 D. Sorigué, K. Hadjidemetriou, S. Blangy, G. Gotthard, A. Bonvalet, N. Coquelle, P. Samire, A. Aleksandrov, L. Antonucci, A. Benachir, S. Boutet, M. Byrdin, M. Cammarata, S. Carbajo, S. Cuiné, R. B. Doak, L. Foucar, A. Gorel, M. Grünbein, E. Hartmann, R. Hienerwadel, M. Hilpert, M. Kloos, T. J.

- Lane, B. Légeret, P. Legrand, Y. Li-Beisson, S. L. Y. Moulin, D. Nurizzo, G. Peltier, G. Schirò, R. L. Shoeman, M. Sliwa, X. Solinas, B. Zhuang, T. R. M. Barends, J. P. Colletier, M. Joffre, A. Royant, C. Berthomieu, M. Weik, T. Domratcheva, K. Brettel, M. H. Vos, I. Schlichting, P. Arnoux, P. Müller and F. Beisson, *Science*, 2021, **372**, eabd5687.
- 33 G. F. Li and K. D. Glusac, *J. Phys. Chem. A*, 2008, **112**, 4573-4583.
- 34 Y. T. Kao, C. Saxena, T. F. He, L. J. Guo, L. J. Wang, A. Sancar and D. P. Zhong, *J. Am. Chem. Soc.*, 2008, **130**, 13132-13139.
- 35 J. Galban, I. Sanz-Vicente, J. Navarro and S. de Marcos, *Methods Appl. Fluoresc.*, 2016, **4**, 19.
- 36 R. A. Marcus and N. Sutin, *Biochim. Biophys. Acta*, 1985, **811**, 265-322.
- 37 C. C. Page, C. C. Moser, X. X. Chen and P. L. Dutton, *Nature*, 1999, **402**, 47-52.
- 38 Samantha J. O. Hardman, Christopher R. Pudney, S. Hay and Nigel S. Scrutton, *Biophys. J.*, 2013, **105**, 2549-2558.
- 39 H. Yang, G. B. Luo, P. Karnchanaphanurach, T. M. Louie, I. Rech, S. Cova, L. Y. Xun and X. S. Xie, *Science*, 2003, **302**, 262-266.
- 40 M. Enescu, L. Lindqvist and B. Soep, *Photochem. Photobiol.*, 1998, **68**, 150-156.
- 41 A. W. MacFarlane and R. J. Stanley, *Biochemistry*, 2003, **42**, 8558-8568.
- 42 G. F. Li, V. Sichula and K. D. Glusac, *J. Phys. Chem. B*, 2008, **112**, 10758-10764.
- 43 J. Brazard, A. Usman, F. Lacombe, C. Ley, M. M. Martin and P. Plaza, *J. Phys. Chem. A*, 2011, **115**, 3251-3262.
- 44 R. K. Zhao, A. Lukacs, A. Haigney, R. Brust, G. M. Greetham, M. Towrie, P. J. Tonge and S. R. Meech, *Phys. Chem. Chem. Phys.*, 2011, **13**, 17642-17648.
- 45 A. Visser, S. Ghisla, V. Massey, F. Muller and C. Veeger, *Eur. J. Biochem.*, 1979, **101**, 13-21.
- 46 T. Okamura, A. Sancar, P. F. Heelis, T. P. Begley, Y. Hirata and N. Mataga, *J. Am. Chem. Soc.*, 1991, **113**, 3143-3145.
- 47 R. Leenders, M. Kooijman, A. Vanhoek, C. Veeger and A. Visser, *Eur. J. Biochem.*, 1993, **211**, 37-45.
- 48 Y. T. Kao, C. Saxena, L. J. Wang, A. Sancar and D. P. Zhong, *Proc. Natl. Acad. Sci. USA*, 2005, **102**, 16128-16132.
- 49 Y. T. Kao, C. Tan, S. H. Song, N. Ozturk, J. Li, L. J. Wang, A. Sancar and D. P. Zhong, *J. Am. Chem. Soc.*, 2008, **130**, 7695-7701.
- 50 J. Li, Z. Y. Liu, C. Tan, X. M. Guo, L. J. Wang, A. Sancar and D. P. Zhong, *Nature*, 2010, **466**, 887-891.
- 51 V. Thiagarajan, M. Byrdin, A. P. M. Eker, P. Müller and K. Brettel, *Proc. Natl. Acad. Sci. USA*, 2011, **108**, 9402-9407.
- 52 S. Ghisla, V. Massey, J. M. Lhoste and S. G. Mayhew, *Biochemistry*, 1974, **13**, 589-597.
- 53 C. T. W. Moonen, J. Vervoort and F. Muller, *Biochemistry*, 1984, **23**, 4859-4867.
- 54 C. T. W. Moonen, J. Vervoort and F. Muller, *Biochemistry*, 1984, **23**, 4868-4872.
- 55 D. A. Dixon, D. L. Lindner, B. Branchaud and W. N. Lipscomb, *Biochemistry*, 1979, **18**, 5770-5775.
- 56 L. H. Hall, M. L. Bowers and C. N. Durfor, *Biochemistry*, 1987, **26**, 7401-7409.
- 57 M. Meyer, H. Hartwig and D. Schomburg, *J. Mol. Struct. (Theochem)*, 1996, **364**, 139-149.
- 58 Y.-J. Zheng and R. L. Ornstein, *J. Am. Chem. Soc.*, 1996, **118**, 9402-9408.
- 59 J. Hahn, M. E. Michel-Beyerle and N. Rosch, *J. Mol. Model.*, 1998, **4**, 73-82.
- 60 C. J. Rizzo, *Antioxid. Redox Signal.*, 2001, **3**, 737-746.
- 61 J. Rodríguez-Otero, E. Martínez-Núñez, A. Peña-Gallego and S. A. Vázquez, *The Journal of Organic Chemistry*, 2002, **67**, 6347-6352.
- 62 Y.-K. Choe, S. Nagase and K. Nishimoto, *J. Comput. Chem.*, 2007, **28**, 727-739.
- 63 R. F. Pauszek, G. Kodali, M. S. U. Siddiqui and R. J. Stanley, *J. Am. Chem. Soc.*, 2016, **138**, 14880-14889.
- 64 K. Schwinn, N. Ferré and M. Huix-Rotllant, *Phys. Chem. Chem. Phys.*, 2020, **22**, 12447-12455.
- 65 B. W. Lennon, C. H. Williams, Jr. and M. L. Ludwig, *Protein Sci.*, 1999, **8**, 2366-2379.

- 66 A. Mees, T. Klar, P. Gnau, U. Hennecke, A. P. M. Eker, T. Carell and L. O. Essen, *Science*, 2004, **306**, 1789-1793.
- 67 R. Dhatwalia, H. Singh, M. Oppenheimer, D. B. Karr, J. C. Nix, P. Sobrado and J. J. Tanner, *J. Biol. Chem.*, 2012, **287**, 9041-9051.
- 68 Y. J. Ai, C. F. Zhao, J. L. Xing, Y. Liu, Z. X. Wang, J. R. Jin, S. H. Xia, G. L. Cui and X. K. Wang, *J. Phys. Chem. A*, 2018, **122**, 7954-7961.
- 69 S. Gozem, E. Mirzakulova, I. Schapiro, F. Melaccio, K. D. Glusac and M. Olivucci, *Angew. Chem. Int. Ed.*, 2014, **53**, 9870-9875.
- 70 J. Bazard, A. Usman, F. Lacombat, C. Ley, M. M. Martin, P. Plaza, L. Mony, M. Heijde, G. Zabulon and C. Bowler, *J. Am. Chem. Soc.*, 2010, **132**, 4935-4945.
- 71 R. Martin, F. Lacombat, A. Espagne, N. Dozova, P. Plaza, J. Yamamoto, P. Muller, K. Brettel and A. de la Lande, *Phys. Chem. Chem. Phys.*, 2017, **19**, 24493-24504.
- 72 F. Lacombat, P. Plaza, M. A. Plamont and A. Espagne, *J. Phys. Chem. Lett.*, 2017, **8**, 1489-1495.
- 73 A. Yoshimura, M. Z. Hoffman and H. Sun, *J. Photochem. Photobiol. A*, 1993, **70**, 29-33.
- 74 K. Ekvall, P. van der Meulen, C. Dhollande, L. E. Berg, S. Pommeret, R. Naskrecki and J. C. Mialocq, *J. Appl. Phys.*, 2000, **87**, 2340-2352.
- 75 I. H. M. van Stokkum, S. L. Delmar and R. van Grondelle, *Biochim. Biophys. Acta Bioenerg.*, 2004, **1657**, 82-104.
- 76 E. R. Henry and J. Hofrichter, *Methods Enzymol.*, 1992, **210**, 129-193.
- 77 P. Hemmerich, C. Veeger and H. C. S. Wood, *Angew. Chem. Int. Ed.*, 1965, **4**, 671-687.
- 78 G. N. Yalloway, S. G. Mayhew, J. P. G. Malthouse, M. E. Gallagher and G. P. Curley, *Biochemistry*, 1999, **38**, 3753-3762.
- 79 M. P. Kabir, Y. Orozco-Gonzalez and S. Gozem, *Phys. Chem. Chem. Phys.*, 2019, **21**, 16526-16537.
- 80 A. H. Steindal, T. T. T. Tam, X. Y. Lu, A. Juzeniene and J. Moan, *Photochem. Photobiol. Sci.*, 2008, **7**, 814-818.
- 81 W. Jarzeba, G. C. Walker, A. E. Johnson, M. A. Kahlow and P. F. Barbara, *J. Phys. Chem.*, 1988, **92**, 7039-7041.
- 82 R. Jimenez, G. R. Fleming, P. V. Kumar and M. Maroncelli, *Nature*, 1994, **369**, 471-473.
- 83 J. Bazard, PhD in Physical and Analytical Chemistry, Université Pierre et Marie Curie, 2009.
- 84 J. Griffin, C. Roshick, E. Iliffe-Lee and G. McClarty, *J. Biol. Chem.*, 2005, **280**, 5456-5467.

FIGURES

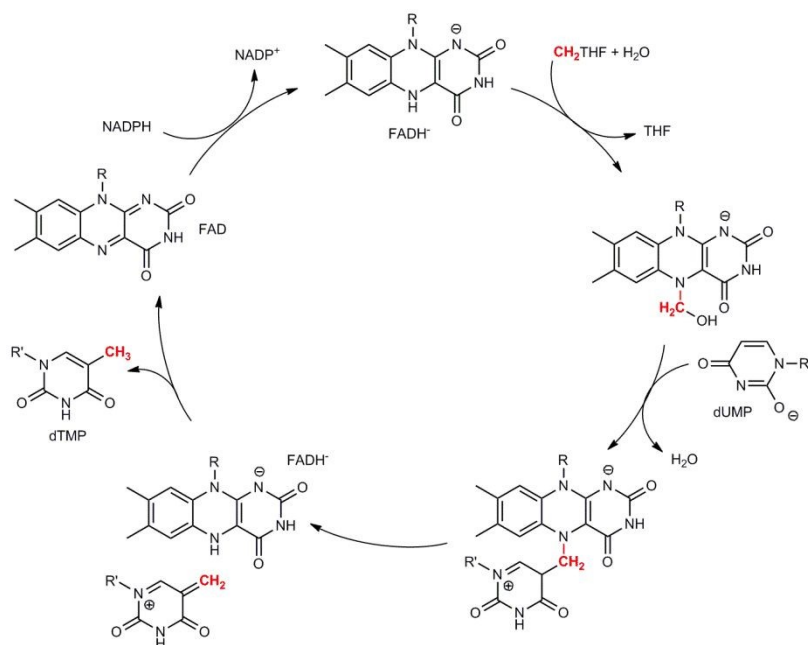


Fig. 1. Catalytic cycle of ThyX. The reduced flavin, FADH⁻, acts as (i) methylene transfer agent between CH₂THF and dUMP via the formation of a flavin carbinolamine species (HO-CH₂-FAD) and as (ii) reducing agent of the exocyclic methylene present on the C₅-dUMP via a hydride transfer to convert it into a methyl group.

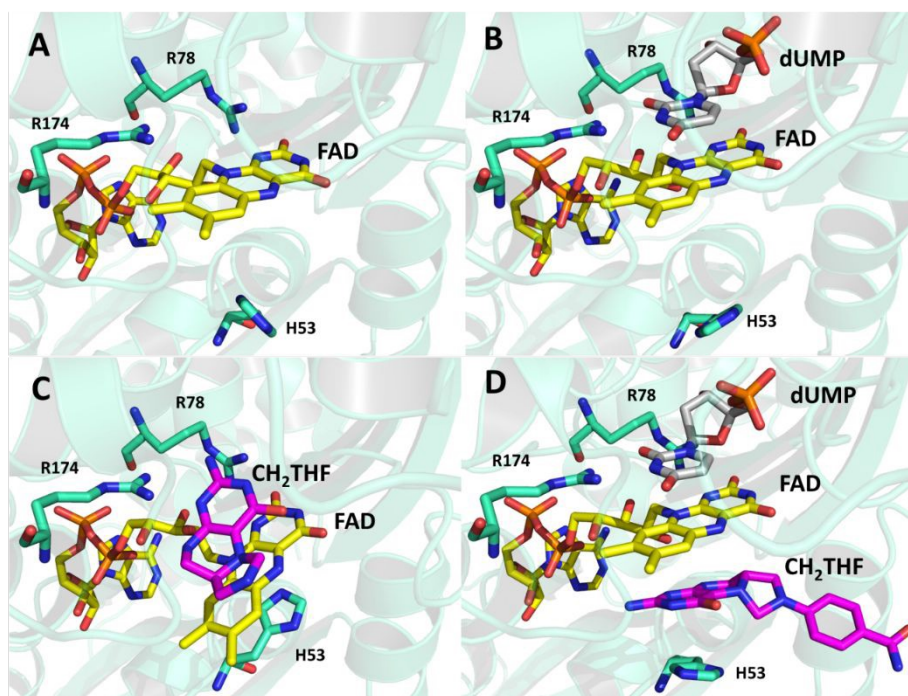


Fig. 2. Crystal structures of oxidized *TmThyX* in four different substrate binding states. A) *TmThyX* free of substrates (pdb: 1O2A). B) *TmThyX* in complex with dUMP (pdb: 1O26). C) *TmThyX* E144R mutant in complex with CH₂THF (pdb: 4GTE). D) *TmThyX* in complex with both dUMP and CH₂THF (pdb: 4GT9). Flavin, dUMP and CH₂THF are shown as yellow, gray and magenta sticks, respectively.

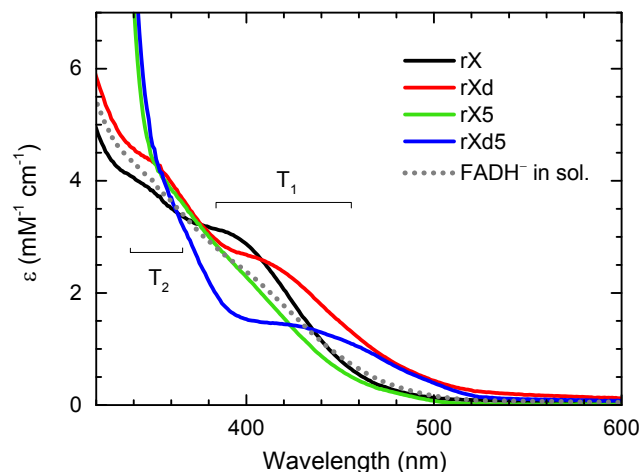


Fig. 3. Steady-state absorption spectra of the four reduced *TmThyX* systems under study: without added substrates (rX; black), with dUMP (rXd; red), with CH₃THF (rX5; green), with dUMP and CH₃THF (rXd5; blue). The spectrum of free FADH⁻ in solution is recalled in dotted line. All spectra are presented in molar extinction coefficient units (ϵ) relative to the flavin concentration. The approximate position of the T₁ and T₂ transitions is indicated.

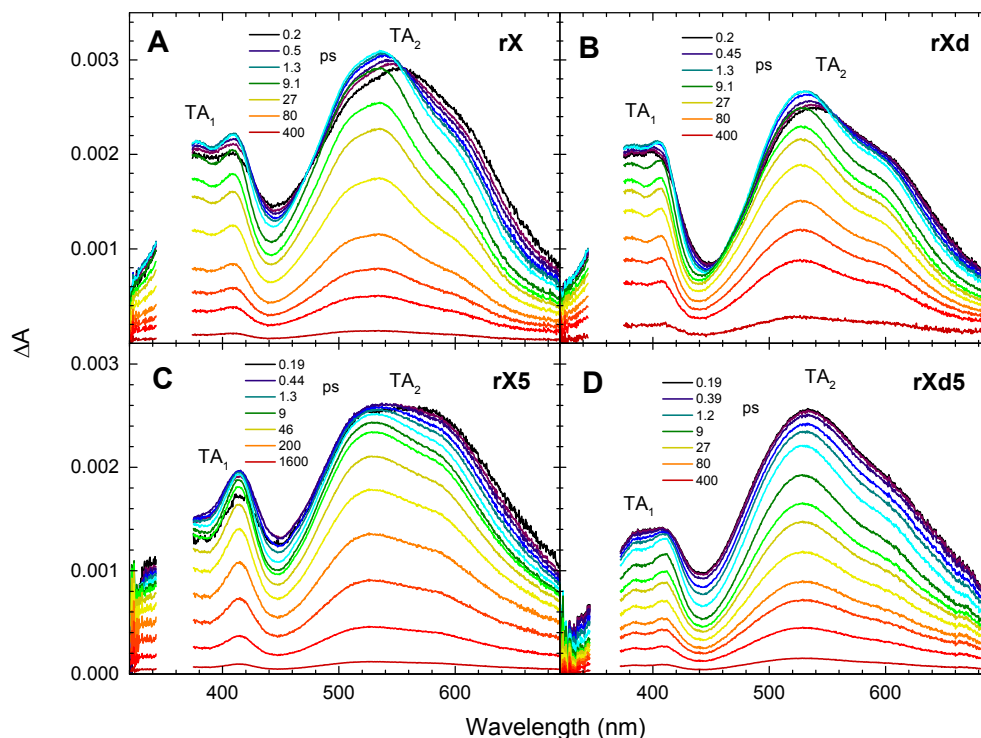


Fig. 4. Femtosecond transient absorption spectra of the four reduced *TmThyX* systems (see notations in Section 3.1) at selected pump-probe delays, with excitation at 360 nm. The approximate position of the TA₁ and TA₂ bands is indicated.

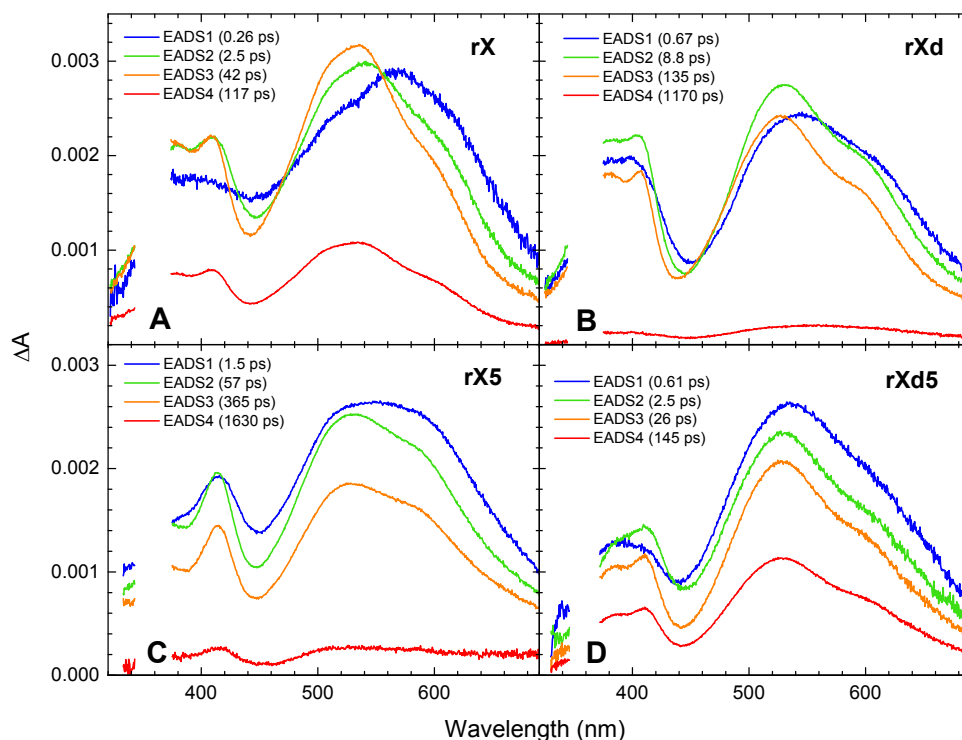


Fig. 5. Evolution-associated difference spectra (EADS) of the four reduced *TmThyX* systems under study (see notations in Section 3.1). In the case of complex *rX*, the small ill-defined plateau (DADS5) has been removed from the calculation of the EADS.

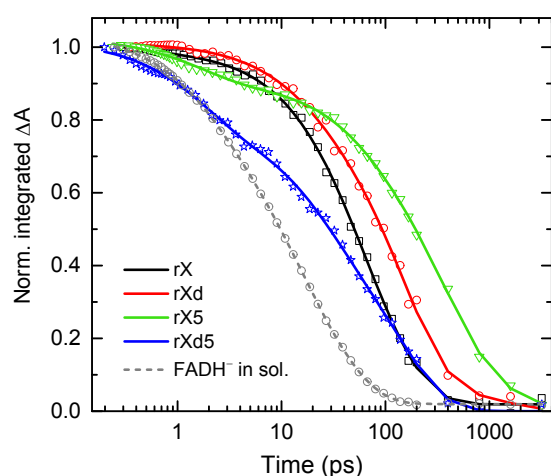


Fig. 6. Normalized integral decay traces of the four reduced *TmThyX* systems under study (symbols). The corresponding multiexponential fits (parameters in Table 2) are shown in continuous lines. The curve in dotted lines refers to free FADH^- in aqueous solution.

Table 1. Time constants (τ_i in ps, with fit errors) of the global multiexponential analysis of the four reduced *TmThyX* systems under study. The last line refers to free FADH⁻ in solution, under the same experimental conditions (ESI, † Section S1).

sample	τ_1 (ps)	τ_2 (ps)	τ_3 (ps)	τ_4 (ps)	plateau
rX	0.26 ± 0.06	2.5 ± 0.4	42 ± 6	117 ± 14	yes
rXd	0.67 ± 0.13	8.8 ± 1.6	135 ± 7	1170 ± 340	no
rX5	1.5 ± 0.2	57 ± 13	365 ± 50	1630 ± 540	no
rXd5	0.61 ± 0.13	2.5 ± 0.5	26 ± 4	145 ± 9	no
FADH ⁻	0.27 ± 0.04	1.5 ± 0.1	8.4 ± 0.7	32 ± 1	yes

Table 2. Time constants (τ_i in ps) of the multiexponential analysis of the integral decay traces. The corresponding relative amplitudes (a_i) and indicated in parentheses. The last line refers to free FADH⁻ in solution.

sample	τ_1 (a_1)	τ_2 (a_2)	τ_3 (a_3)	τ_4 (a_4)	plateau
rX	0.38 (0.02)	41 (0.41)	114 (0.55)	–	(0.02)
rXd	17 (0.13)	148 (0.80)	1330 (0.07)	–	–
rX5	1.6 (0.12)	63 (0.14)	375 (0.60)	1680 (0.14)	–
rXd5	1.6 (0.22)	22 (0.26)	143 (0.52)	–	–
FADH ⁻	2.0 (0.21)	10.9 (0.35)	35 (0.42)	–	(0.02)

Table 3. Average decay time ($\bar{\tau}$) and standard deviation of decay times (σ) calculated from the multiexponential fit of the integral decay traces (see ESI, † Section S1.3). The ratios of $\bar{\tau}$ relative to free FADH⁻ are provided in the last column.

sample	$\bar{\tau}$ (ps)	σ (ps)	$\bar{\tau}/\bar{\tau}_{ref}$
rX	81	38	4.2
rXd	218	317	11
rX5	464	504	24
rXd5	80	65	4.2
FADH ⁻	19.2	13.8	1

ASSOCIATED CONTENT

Supplementary information available:

AUTHOR INFORMATION**Corresponding Authors**

*Pascal Plaza: Email: pascal.plaza@ens.fr. Phone: +33 144322414.

*Djemel Hamdane: Email: djemel.hamdane@college-de-france.fr. Phone: +33 44271254.